

TRANSMISSION X-RAY DIFFRACTION (XRD) PATTERNS RELEVANT TO THE MSL CHEMIN AMORPHOUS COMPONENT: SULFATES AND SILICATES. R.V. Morris¹, E.B. Rampe², T.G. Graff³, P.D. Archer, Jr.³, L. Le³, D.W. Ming¹, and B. Sutter³. ¹NASA-JSC, Houston, TX 77058, richard.v.morris@nasa.gov. ²Aerodyne Industries, Jacobs-JETS, Houston, TX 77058, ³Jacobs, NASA-JSC, Houston, TX 77058.

Introduction and Background: The Mars Science Laboratory (MSL) CheMin instrument on the Curiosity rover is a transmission X-ray diffractometer (Co-K α radiation source and a $\sim 5^\circ$ to $\sim 52^\circ$ 2θ range) where the analyzed powder samples are constrained to have discrete particle diameters $<150\ \mu\text{m}$ by a sieve [1]. To date, diffraction patterns have been obtained for one basaltic soil (Rocknest (RN)) and four drill fines of coherent rock (John Klein (JK), Cumberland (CB), Windjana (WJ), and Confidence Hills (CH)) [2-4]. The CheMin instrument has detected and quantified the abundance of both primary igneous (e.g., feldspar, olivine, and pyroxene) and secondary (e.g., Ca-sulfates, hematite, akaganeite, and Fe-saponite) minerals [2-5]. The diffraction patterns of all CheMin samples are also characterized by a broad diffraction band centered near $30^\circ\ 2\theta$ and by increasing diffraction intensity (scattering continuum) from $\sim 15^\circ$ to $\sim 5^\circ$, the 2θ minimum.

Both the broad band and the scattering continuum are attributed to the presence of an XRD amorphous component. Estimates of amorphous component abundance, based on the XRD data itself [2,4] and on mass-balance calculations using APXS data crystalline component chemistry derived from XRD data, martian meteorites, and/or stoichiometry [e.g., 6-9], range from $\sim 20\ \text{wt.}\%$ to $\sim 50\ \text{wt.}\%$ of bulk sample. The APXS-based calculations show that the amorphous component is rich in volatile elements (esp. SO_3) and is not simply primary basaltic glass, which was used as a surrogate to model the broad band in the RN CheMin pattern [2]. For RN, the entire volatile inventory (except minor anhydrite) is assigned to the amorphous component because no volatile-bearing crystalline phases were reported within detection limits [2]. For JK and CB, Fe-saponite, basanite, and akaganeite are volatile-bearing crystalline components.

Here we report transmission XRD patterns for sulfate and silicate phases relevant to interpretation of MSL-CheMin XRD amorphous components.

Samples and Methods: For sulfate experiments, 10 acid-sulfate solutions were prepared from standard reagents (Table 1). Cryoprecipitation (precipitation by removing water as ice) was induced by freezing solutions using liquid N_2 . After freeze drying, the precipitates were stored in closed containers in a glove box purged with dry- N_2 gas. For silicate experiments, silicate liquids having compositions equivalent to representative MER rocks and soils (SO_3 - and Cl -free) [e.g., 10, 11] were equilibrated at 1350 - 1450°C in a 1-atm gas mixing furnace at IW+1 oxygen fugacity and

quenched in water to room temperature. Transmission XRD diffraction patterns were obtained on a CheMin-4 diffractometer which is a laboratory version of the MSL CheMin instrument. Dry N_2 purge gas was used for the sulfate measurements.

Table 1. Compositions of Starting Acid-Sulfate Solutions for Cryoprecipitation of Sulfates

Cation(s)	Concentration (M)	Volume (mL)	Cation Ratio
Fe^{3+}	1.00	20	---
Fe^{2+}	1.00	15	---
Mg^{2+}	1.00	20	---
Ca^{2+}	0.015	500	---
K^+	0.50	40	---
Na^+	0.25	100	---
$\text{Fe}^{2+}, \text{Mg}^{2+}$	0.5, 0.5	20	1:1
$\text{Fe}^{3+}, \text{Mg}^{2+}$	0.5, 0.5	40	1:1
$\text{Fe}^{2+}, \text{Ca}^{2+}$	0.015, 0.015	500	1:1
$\text{Fe}^{3+}, \text{Mg}^{2+}, \text{K}^+, \text{Na}^+$	0.2, 0.2, 0.02, 0.02	100	10:10:1:1

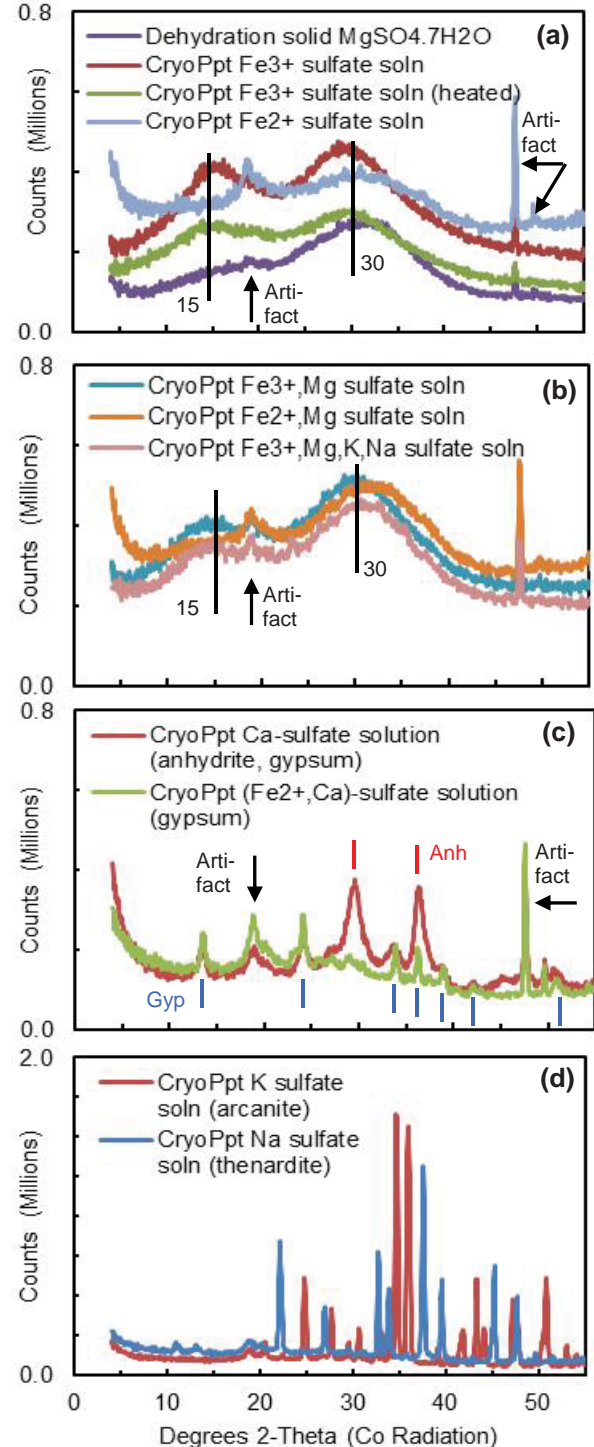
Results: Single and mixed cation sulfate solutions of Mg^{2+} , Fe^{2+} , and Fe^{3+} in any proportion are likely capable of forming amorphous products by cryoprecipitation (Fig. 1a,b). Single cation Ca^{2+} , K^+ , and Na^+ sulfate solutions did not form amorphous precipitates (anhydrite plus gypsum, arcanite, and thenardite, respectively, with gypsum the only hydrated sulfate), and neither did a solution with $\text{Fe}^{2+}:\text{Ca}^{2+}=1:1$ (Fig. 1c,d), although only gypsum was detected. However, a solution with $\text{Fe}^{3+}:\text{Mg}^{2+}:\text{Na}^+:\text{K}^+ = 10:10:1:1$ formed an XRD amorphous precipitate (Fig 1b.). Additional experiments will define the compositions over which mixed cation sulfate solutions produce amorphous and mixed amorphous-crystalline precipitates. Especially relevant are sulfate solutions involving Ca^{2+} , because crystalline Ca-sulfates are detected by CheMin [2,4].

In general, amorphous sulfates have a broad intensity maximum near $\sim 30^\circ\ 2\theta$ and another one with less intensity at lower 2θ (Fig. 1a,b). Their overall shapes and 2θ locations (esp. Mg^{2+} and/or Fe^{2+} compositions) are not inconsistent with CheMin results, e.g., compare with basaltic soil glass (Fig. 2a) which was used by [2] for RN amorphous calculations. However, a quantitative analysis has not been done.

With one exception, the silicate glasses were predominantly amorphous with a single broad diffraction feature whose peak position increased from $\sim 25^\circ$ to $\sim 31^\circ\ 2\theta$ with increasing SiO_2 (Fig 2a). The Mg-rich composition (Algonquin) produced forsterite plus the most SiO_2 -poor glass as indicated by the maximum

diffraction intensity at $\sim 34^\circ 2\theta$ (Fig. 2b). The diffraction pattern of the high-SiO₂ residue of acid-sulfate leached terrestrial basaltic tephra (HWMK051) has a diffraction maximum ($\sim 26^\circ 2\theta$) just longward of that for commercial SiO₂ glass ($\sim 25^\circ 2\theta$) (Fig. 2c).

Our results show that the shape and position of the amorphous component of MSL CheMin data may, at least semiquantitatively, fingerprint its nature.



References: [1] Blake et al. (2012) *SSR*, DOI 10.1007/s11214-11012-19905-11211. [2] Bish et al. (2013) *Science*, 341, DOI:10.1126/science.1238932. [3] Blake et al. (2013) *Science*, 341, DOI:10.1126/science.1239505. [4] Vaniman et al., (2013) *Science*, 343 DOI:10.1126/science.1243480. [5] Treiman et al. (2014) *Am. Min.*, 99, 2234. [6] Morris et al. (2013) *LPSC44*, abs. #1653. [7] Morris et al. (2014) *LPSC45*, abs.#1319. [8] Dehouck et al. (2014) *JGR*, 10.1002/2014JE004716. [9] Morris et al. (2015) *LPSC46*, this volume. [10] Ming et al. (2008) *JGR*, 113, E12S39, doi:10.1029/2008JE003195. [11] Morris et al. (2008) *JGR*, 113, E12S42, doi:10.1029/2008JE003201.

Fig. 1 (left). XRD patterns of cryoprecipitated single and mixed cation acid sulfate solutions and rapid dehydration of solid MgSO₄.7H₂O (same as cryoprecipitation).

Fig. 2 (below). XRD patterns of (a) commercial SiO₂ glass and MER-composition (SO₃⁻ and Cl-free) silicate liquids quenched from 1350-1450°C and IW+1 oxygen fugacity, (b) similarly quenched Algonquin liquid with olivine and glass, and (c) high-SiO₂ residue of basalt leached under natural acid sulfate conditions (HWKV051) compared to SiO₂ and Adirondack glasses.

